Optimization of Surface Roughness and Diameter Error in Thin-Walled AA6063 during Internal Turning under Minimum Quantity Lubrication

Albertus Rianto Suryaningrat[1,2], Arif Wahjudi[1,*], Suhardjono[1], Muizuddin Azka[2]

[1]Department of Mechanical Engineering, Faculty of Industrial Technology and Systems Engineering Institut Teknologi Sepuluh Nopember, Surabaya 60111, Indonesia
[2]Research Center for Manufacturing Technology of Production Machinery National Research and Innovation Agency, Jakarta 10340, Indonesia

*Author to whom correspondence should be addressed:
E-mail: arif_w@me.its.ac.id

(Received May 28, 2025; Revised November 10, 2025; Accepted December 07, 2025)

Abstract: Thin-walled aluminum alloy 6063 (AA6063) components are commonly used in landing gear manufacturing through internal turning. However, tool and workpiece deflection cause diameter errors, altering the depth of cut, inducing chatter, and degrading surface finish. While cutting fluids reduce friction and vibration, conventional mineral oils harm the environment. This study employed the Taguchi L9 (3^3) design and the Multi-Response Performance Index (MRPI) to optimize internal turning under minimum quantity lubrication (MQL) using virgin coconut oil (VCO). MRPI combines surface roughness and diameter error into a single index for parameter selection. The optimal settings—depth of cut 0.8 mm, feed rate 0.075 mm/rev, and cutting speed 200 m/min—yielded 4.72 µm surface roughness and 0.09 mm diameter error, demonstrating that MQL with VCO enhances machining quality and supports sustainable manufacturing.

Keywords: green manufacture; internal turning; MQL; surface roughness; thin-walled

1. Introduction

Turning machining is one of the most commonly used methods for processing cylindrical parts. Advances in CNC turning machine technology have enabled precise motion control through G-code programing. Machining parameters such as depth of cut (a_p), feed rate (f), and cutting speed (v_c) are critical inputs for the operators during the programing configuration. The selection of cutting parameters, particularly the feed rate, significantly improves the surface roughness (SR) quality[1)]. However, setting these parameters is a dilemma because improving the surface quality often conflicts with efforts to increase production rates. Therefore, an optimal balance between these 2factors is essential to achieve the desired outcome.
During the machining of thin-walled components, the selection of machining parameters is essential for improving the SR and the geometric precision of the part. This research was motivated by a case study on the production of shock absorber components for landing gear and serves as the foundation for the current investigation. SR on the inner cylinder surface is a significant concern because it can cause micro-gaps that can lead to leakage, thereby affecting the component's performance. The material used is aluminum alloy AA-6063, chosen for its capability to achieve smooth surface finishes and its compatibility with anodizing processes[2,3)]. AA-6063 provides several benefits in producing high-quality surfaces, with a Vickers hardness of 50.36 kg/mm³, ultimate tensile strength of 130 MPa, and an elongation of 23%[4)]. Diameter error (ED) is another critical challenge that affects dimensional accuracy and the fit of components during assembly[5)], particularly in thin-walled structures[6)], where low stiffness further exacerbates the difficulty in maintaining precision.
Internal turning employs a boring bar as the tool holder, with a higher overhang-to-diameter (L/D) ratio compromising its rigidity[7)]. However, the tool holder's consistent stiffness, is undermined by thin-walled components, which exhibit low workpiece stiffness, leading to axial deflection, uneven chip thickness, and incomplete material removal[6)]. Dynamic factors, such as chip thickness fluctuations, also induce chatter during machining, which alters cutting force (Fc) and generates

Cite: A. Rianto et al., "Optimization of Surface Roughness and Diameter Error in Thin-Walled AA6063 during Internal Turning under Minimum Quantity Lubrication". Evergreen, 13 (01) 373-386 (2026). https://doi.org/10.5109/7411072.

vibration[8]. This interaction between the workpiece and boring bar reduces process stability[9]. Chatter increases SR, tool wear, and energy consumption[10]. Although reducing depp of cut (a_p) and cutting speed (v_c) can minimize chatter, it also lowers productivity[11]. Using cutting fluid helps enhance machining stability[12].

Green manufacturing focused on sustainability has become central in Life Cycle Assessment (LCA) research[13,14]. In metal cutting, cutting fluids reduce friction, prevent BUE, improve SR[17] and dimensional accuracy[15]. Virgin coconut oil (VCO) provides good durability and effectively reduces chatter[12,16–18]. To minimize fluid consumption, the minimum quantity lubrication (MQL) method, which combines VCO with compressed air and sprays it as a mist[16], has been increasingly adopted. This method eliminates the need for coolant storage and helps reduce bacterial risks[19].

Several studies have examined the turning process of thin-walled components, focusing on modeling[20], parameter selection[21,22], cutting-force analysis[23], tool life[22,24], vibrations[25], and surface topography[6]. However, few studies have explored internal turning, which presents more complexity due to static and dynamic deflections caused by variations in cutting force (Fc). Static forces cause geometric errors, such as diameter inaccuracies[6,26], while dynamic forces lead to vibrations and chatter[27], resulting in uneven SR and inconsistent tool marks.

Multi-objective optimization is used to simultaneously optimize multiple objectives, such as ED and SR. This study aims to optimize these using the Multi-Response Performance Index (MRPI), which was chosen for its simplicity and ease of interpretation. Unlike Taguchi–Grey Relational Analysis (T-GRA)[28], MRPI does not require complex computations or weight assignments, thereby avoiding potential bias. MRPI relies on performance ratios relative to a reference value, thereby simplifying the process without needing explicit normalization. The sensitivity of the T-GRA is generally higher than that of the T-MRPI approach. T-GRA achieves this by evaluating the relative closeness of each response to an ideal reference through normalization, thereby increasing its responsiveness to small variations among multiple responses. In contrast, T-MRPI combines the signal-to-noise (S/N) ratios of all responses into a single index, which simplifies computation but reduces its ability to detect subtle changes in individual responses. The RSM–MRPI approach demonstrates moderate to high sensitivity, primarily due to the continuous nature of RSM modelling, which effectively captures small variations and interactions among process parameters. effectiveness of MRPI, because MRPI integrates multiple responses into a single index, its overall sensitivity may still be lower than that of RSM–desirability or T-GRA. In contrast to the Technique for Order of Preference by Similarity to Ideal

Table 1: Multi-Objective Optimization in Turning Process

Reference	Methods	Material and Process Parameter	Response Parameter
Imran (2025) [32]	GRA vs DEAR (MRPI) vs MOORA	Wet & Dry Ext-Turning – Mild Steel, a_p, v_c, f, n	3D- morphology (Sa, Sz, Sq), MRR
Gopi (2025)[33]	DEAR (MRPI) - MOGWO	MQL- Ext-Turning – AA2014, a_p, v_c, f	MRR, RA
Mastan (2024) [34]	T-GRA vs T-TOPSIS	Dry Ext-Turning - Inconel 718, a_p, v_c, f	SR, T_w, MRR
Vieira (2024) [35]	RSM-NSGA-II	Dry Int-Turning - PEEK, v_c, f, fixing position	SR, F_c, MRR, Roundness
Fan (2024) [36]	GA-ANN and RSM(ccd)-ANN	Dry Int-Turning – Glass, a_p, v_c, f, Laser Power	SR, F_{result}.
Sahin (2024) [37]	RSM(Box) - MRPI	Dry Ext-Turning – AISI 1040, a_p, v_c, f	SR, MRR
Tura (2024) [38]	GA-RSM and vs T-GRA	Dry Ext-Turning – AISI D2, a_p, v_c, f	SR, F_c
Evanovich (2022)[39]	DEAR (MRPI) vs GRA vs TOPSIS	Dry Ext-Turning -– Inconel 718, a_p, v_c, f, r (radius of tool)	Ra, Vb, MRR
Safi (2022)[40]	GRA vs MOORA vs DEAR vs WASPAS	Dry Ext-Turning – Tool Steel, a_p, v_c, f, r (radius of tool)	Ra, MRR, Fz (Force Axial), Pc (Power)
Chate (2021)[41]	T-DEAR (MRPI) vs T-MOORA	Dry Ext-Turning – Mild Steel, a_p, v_c, f	SR, MRR, CE (Circularity Error)
Kalyanakumar (2021) [42]	T-GRA	Dry Ext-Turning – EN24T, a_p, v_c, fr, type coolant	SR, Tw, MRR, Roundness
Sarma (2021) [43]	RSM(Box)-MRA	MQL Ext-Turning - TiA, v_c, f, angle, type fluid	SR, F_c, T_c, T_w
Moganapriya (2021)[44]	T-DEAR (MRPI)	Dry Ext-Turning -AISI 420, a_p, v_c, f,	SR, Vb, MRR
Lakshmi V (2020)[45]	DEAR (MRPI)	MQCL - Ext-Turning - Ti-6Al-4V, a_p, v_c, f	SR, MRR, T_{wr} (Wear Rate), Vib

Solution (TOPSIS), which ranks options based on their proximity to an ideal solution[29]. MRPI also sidesteps the complexity of algorithms like Genetic Algorithms (GA)[30] and metaheuristic methods such as Multi-Objective Particle Swarm Optimization (MOPSO)[31]. However, the effectiveness of MRPI can decrease with an increasing number of variables and data uncertainty. Table 1 shows several literature reviews that use multi-objective optimization in the turning process, employing various methods with MRPI, with few focusing on internal turning, and none examining thin-walled structures. This study aims to optimize the cutting parameters for multiple responses, specifically SR and ED based on a case study of shock absorber production for landing gear, where both SR and ED are critical for product quality. MRPI is employed to optimize SR and ED during internal turning of thin-walled AA-6063 under MQL-VCO. The study focuses on the underexplored aspect of ED, particularly in the internal turning of thin-walled structures. Key contributions include:

Analyzing the impact of cutting parameters on SR and ED during the internal turning of Thin Wall AA-6063 using MRPI.

Assessing the feasibility of MQL-VCO to enhance SR and ED.

2. Methods

2.1. Taguchi Method

The Taguchi method differentiates the experimental results from the desired values by employing a loss function. This loss function serves as the foundation for developing the signal-to-noise (S/N) ratio, which is designed to evaluate the quality of a process or system[46]. The S/N ratio integrates the signal data (S), which represent the desired influence on the test results, and noise data (N), which reflect undesired influences. Consequently, a higher S/N ratio indicates better performance because it signifies the optimization of the desired signals and minimization of the noise effects. There are 3 main approaches to calculating the S/N ratio: the smaller-the-better, nominal-the-best, and larger-the-better methods, each applied based on the characteristics of the parameters being analyzed.

In this study, the smaller-the-better approach was used to determine the optimal combination for SR and ED. The larger-the-better approach was applied after converting the multi-response data into single-response data. The formulas[34] for the smaller-the-better and larger-the-better approaches are as follows.

Smaller-the-better (minimize):

$$S/N = -10log\left(\frac{1}{n}\sum_{i=1}^{n} Y_1^2\right). \quad (1)$$

Larger-the-better (maximize);

$$S/N = -10log\left(\frac{1}{n}\sum_{i=1}^{n}\frac{1}{Y_1^2}\right). \quad (2)$$

Where Y_i represents the machining response characteristic for the n-th experimental condition. The negative sign in Eq.(1) and Eq.(2) is used solely to indicate the characteristics of the smaller-the-better and larger-the-better approaches.

2.2. Multi-Response Optimization

The Taguchi method is primarily designed to optimize a single response or dependent variable. In this approach, the optimal parameters are determined by analyzing the mean or maximum value of the average signal-to-noise (S/N) ratio, which is specifically tailored for handling single-response problems. The Taguchi method cannot be directly applied to the optimization of multi-response problems. In the weighting method, multi-response problems are transformed into single-response problems.

$$MRPI = W_{ED} * Y_{ED} + W_{SR} * Y_{SR}. \quad (3)$$

In Eq (3) [37], the Multi-Response Performance Index (MRPI) is used to transform a multi-response problem into a single-response problem. In Eq (4) and Eq (5)[37], The S/N ratio for the weight (W) and response (Y) of the *i*-th experimental condition was calculated using the smaller-is-better approach.

$$W_{ED_i} = \frac{\left(\frac{1}{Y_{ED_i}}\right)}{\left(\sum\frac{1}{Y_{ED}} + Y_{ED_i}\right)}. \quad (4)$$

$$W_{SR_i} = \frac{\left(\frac{1}{Y_{SR_i}}\right)}{\left(\sum\frac{1}{Y_{SR}} + Y_{SR_i}\right)}. \quad (5)$$

2.3. Experiment Setups

The use of Taguchi L_9 (3^3) orthogonal arrays requires an optimal range-level parameter selection approach. The tool used was a CNMG120408AH-KW10 made by Kyocera, specifically recommended for nonferrous materials. The turning process was conducted using a CNC-LEADWELL-T6 with a spindle power of 5.5 kW, and a steel S25L-MCLNR12 boring bar. The cutting tool manufacturer's recommendations for the material being machined were considered during the preliminary trials. The parameter levels were adjusted according to the stiffness of the boring bar and workpiece. The experimental design is presented in Table 2.

Table 2: Design of experiment by Taguchi $L_9(3^3)$

Cutting Parameters	Notation	Unit	Level		
			1	2	3
Depth of cut	a_p	mm	0.3	0.6	0.8
Feed Rate	f	mm/rev	0.050	0.075	0.10
Cutting Speed	v_c	m/min	150	200	250

Table 3: Experimental Layout *L9* Orthogonal Array

Exp. No.	Cutting Parameter Level		
	a_p	f	v_c
1	1	1	1
2	1	2	2
3	1	3	3
4	2	1	3
5	2	2	1
6	2	3	2
7	3	1	2
8	3	2	3
9	3	3	1

Table 3 presents the experimental layout design based on the Taguchi $L_9(3^3)$ orthogonal array method.

The data collection procedure was carried out as follows:

The workpieces were tested using an OES spectrometer and categorized as AA-6063 (see in Table4), The machinability and mechanical properties follow the reference[4]. Each workpiece has an outer diameter of 88.9 mm, an inner diameter of 79.9 mm, an initial wall thickness of 4.5 mm, and a material length of 150 mm. The geometric profile of the finished product, with a final wall thickness of 3 mm, is shown in Figure 1.

The workpiece was clamped along a length of 3.5 mm using a 3-hard jaw chuck, with an overhang of approximately ±110 mm on the raw material. A run-out test was conducted during installation to ensure balanced rotation of the workpiece, with radial deviation not exceeding 0.25 mm and axial deviation not exceeding 0.2 mm.

The boring bar had installed with an overhang of approximately ±125 mm, resulting in L/D ratio of approximately 5.

An external turning process was used to ensure that the testing was conducted on a uniform wall thickness. The geometric profile of the finished product is shown in Figure 1.

Pre-machining was performed in accordance with the design of experiments (DOE) outlined in Table 3. To ensure the use of a fresh cutting edge, the cutting insert was replaced between the pre-machining and finishing processes. For consistency, the workpiece and the boring bar were not removed during data collection.

According to the literature review[47], MQL using vegetable-based cutting oil is suitable for a flow rate of 150 ml/min with an air pressure of 3 bar in the outer turning process. Unlike in outer turning, in internal turning, the cutting oil is retained on the inner surface of the cylinder. In this experiment, the MQL system was configured with a flow rate of 30 ml/min and an air pressure of 30 psi (2 bar). The lubricant spray was directed toward the rake surface of the cutting insert to facilitate chip breaking and prevent the formation of BUE. The experimental setup is show in Figure 2.

Vibration data acquisition was performed using a Dytran-3413A2 accelerometer, the experiment modal analysis (EMA) used a Dytran-5800B3 impact hammer and data acquisition used a Yokogawa DL-750 oscilloscope. The accelerometer was positioned 10 mm from the fixture, as illustrated in Figure 2. and a sampling rate of 5 kHz was used. The sensitivity of the accelerometer was 5.18 mV/(m/s²), and the sensitivity of the impact hammer is 11.07 mV/N.

SR measurements were carried out using a Mitutoyo SJ-301 across 3 planes, spaced at angular intervals of ±120° (A, B, C), and at five different depths: 0–20 mm (1), 21–40 mm (2), 41–60 mm (3), 61–80 mm (4), and 81–100 mm (5), as shown in Figure 3. A total of 15 measurement points were taken for each experiment. The stylus was oriented perpendicular to the cutting path during the measurements. The probe sensitivity for the SR measurement is 10 µm/cm in the vertical direction and 500 µm/cm in the horizontal direction. Each measurement was repeated 3 times, and the best value was recorded. For the SR response analysis, the SR value at the free end was utilized, while measurements across the 5 planes were performed to observe tapering phenomena. The SR testing on the cutting test was conducted on a flat granite table as shown in Figure 5 (a).

ED measurements were conducted using a Coordinate Measuring Machine (CMM) equipped with a stylus probe of 2 mm diameter and 35 mm length as shown in Figure 5 (b). The sensitivity of the CMM is ± 0.1 µm and the sensitivity of the probe is 0.1 µm per trigger. Measurements were performed in 3 planes, with the first plane (D1) located 2 mm from the free end. Subsequent measurements were taken at 2 additional depths, 10 mm (D2) and 20 mm (D3), as shown in Figure 4. The measurement process was conducted with 20 points (hits) on the same plane, and the measurement was repeated once on a different plane. Based on the literature review, the residual material resulting from the thin-walled phenomenon was observed, and the measured diameter values to consistently fall below the expected diameter (Dd) of 82.2 mm.

To examine the surface morphology of the machined samples under both MQL and dry conditions, a JEOL JSM-6510LA scanning electron microscope (SEM) was employed. The magnification level was carefully adjusted to obtain clear micrographs with adequate resolution for detailed interpretation and analysis.

Table 4: Chemical composition of the workpiece

Al	Si	Mg	Fe	Cu	Cr	Zn	Mn	Ti
98.9	0.413	0,508	0,219	0,002	0,001	0,015	0,003	0,009

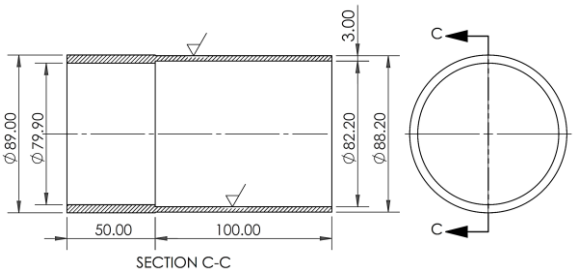

Fig. 1: Geometric cutting test

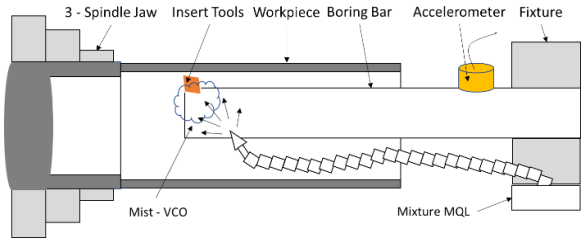

(a) Illustration of experimental setup

(b) Internal turning under MQL

Fig. 2: Experimental Setup

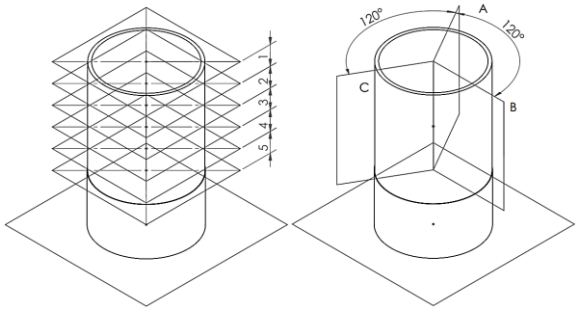

Fig. 3: Illustration of the plane used for measuring SR

3. Results and Discussion

The raw material AA-6063 used exhibited varying circularity errors for each specimen. The material was suspected to be bent due to improper material handling during transportation by the delivery service.

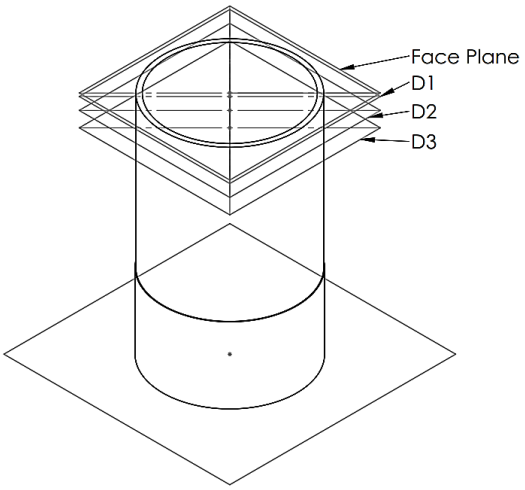

Fig. 4: Illustration of the plane used for measuring the ED

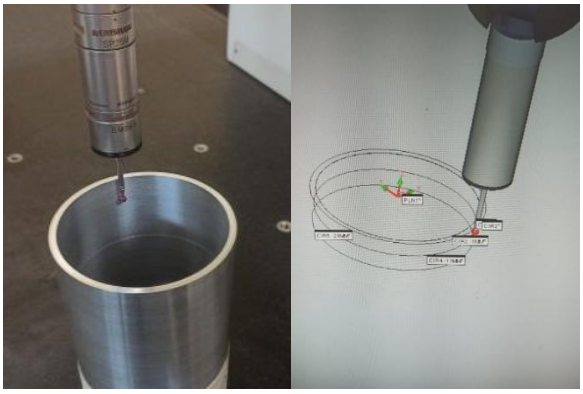

(a) ED measurement with CMM Brown & Sharpe

(b) SR measurement using Mitutoyo SJ-301

Fig. 5: Measurement Instrument

3.1. Surface Roughness Testing

The measurement results are presented in Figure 6 indicates that Exp.01 achieved the optimal SR. The SR for each plane exhibited an upward trend with increasing measurement depth, although the values were not consistently uniform. The data presented are the average results of 3 measurements taken at different angular direction, as shown in Figure 3.

The average SR values measured at a depth of 0–20 mm were used as the response data for the analysis. Subsequently, a Taguchi main effect analysis was performed, and the results are presented in Figure 7. The contour plot shown in Figure 8 illustrates the relationship between feed rate (f) and depth of cut (ap) in relation to SR. The SR decreases with higher feed rates and depth of cut, indicating that these parameters significantly influence the surface quality of the workpiece.

Table 5 presents the ANOVA results, indicating that each parameter (a_p, f, and v_c) has 2 degrees of freedom. The total variation is represented by the adjusted sum of squares, and the mean square values are obtained by dividing these by the respective degrees of freedom. A higher F-value suggests a stronger influence of the factor on the response variable. Parameters with P-values less than 0.05 were considered statistically significant. The percentage contribution shows the extent to which each factor affects

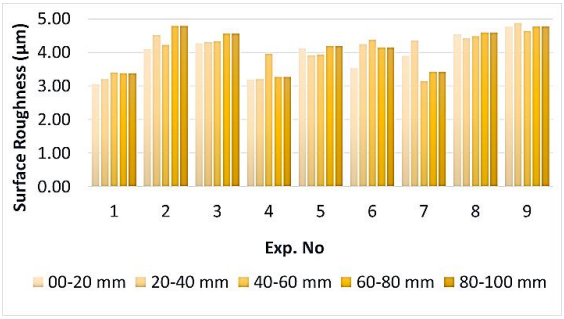

Fig. 6: Result of the Surface Roughness (*SR)*

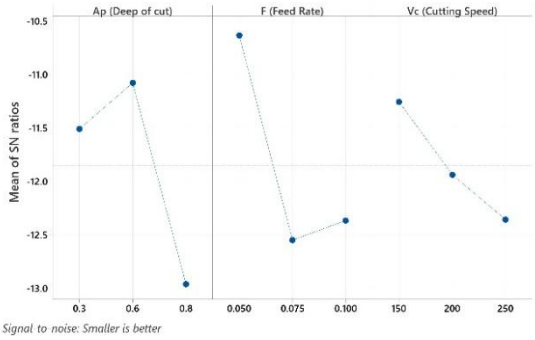

Fig. 7: Main Effect Plot for S/N Ratios with SR

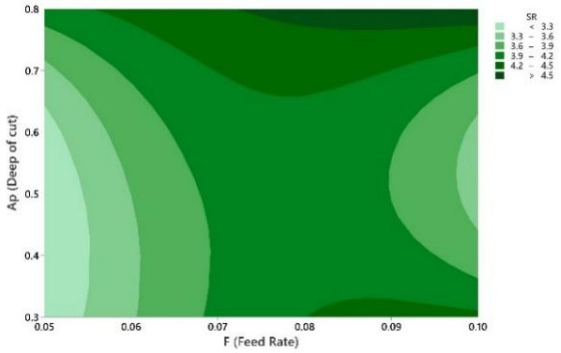

Fig. 8: Contour Plot of SR vs a_p vs f

Table 5: ANOVA and percentage contributions for SR

Source	DF	Adj SS	Adj MS	F	P	% Cont.
a_p	2	1.196	0.598	78.3	0.01	43.4
f	2	1.233	0.616	80.7	0.01	44.7
v_c	2	0.309	0.154	20.2	0.04	11.2
Error	2	0.015	0.007			0.55
Total	8	2.753				100

the total variation, with higher values indicating a more dominant impact on the response. The table shows that the feed rate (f) has the factor with the highest contribution to the response variance, representing 44.77 % of the total variance. Furthermore, the factors depth of cut (a_p), feed rate (f), and cutting speed (v_c) were statistically significant, as indicated by P-values less than 0.05. The error variance (SS) is minimal at 0.56%, indicating that the model provides a good fit to the observed data.

3.2. Error Diameter Testing

The ED is defined as the deviation between the desired diameter (Dd) of 82.2 mm and the measured diameter (Di). As shown in Figure 9, the optimal ED value was obtained in Exp.02. Furthermore, the ED values at the 3 depths, as illustrated in Figure 4, exhibited a tendency toward tapering.

The ED measurements were conducted at a depth range of 0–10 mm, with 3 repetitions performed on the same plane to ensure accuracy. The Taguchi main effect analysis was performed using the average ED values from these measurements, as shown in Figure 10. The contour plot shown in Figure 11 demonstrates the

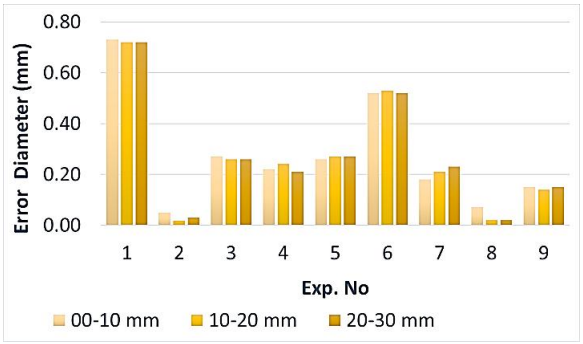

Fig. 9: Result of the Diameter Error (*ED*)

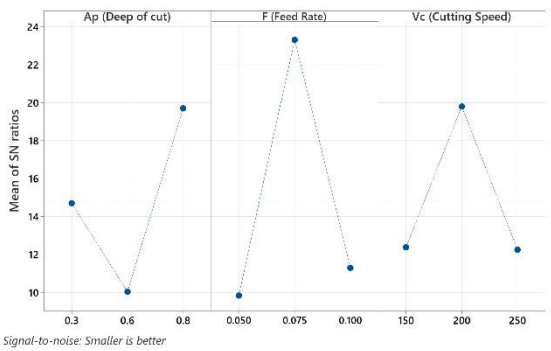

Fig. 10: Main Effect Plot for S/N Ratios with ED

Cite: A. Rianto et al., "Optimization of Surface Roughness and Diameter Error in Thin-Walled AA6063 during Internal Turning under Minimum Quantity Lubrication". Evergreen, 13 (01) 373-386 (2026). https://doi.org/10.5109/7411072.

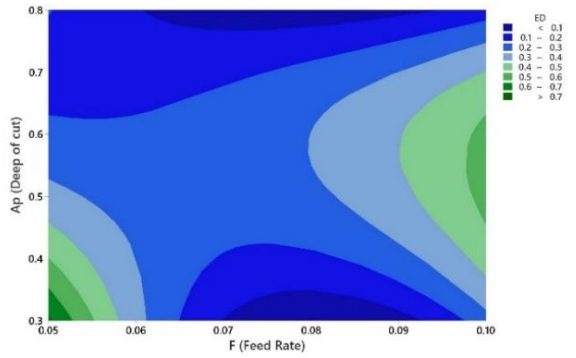

Fig. 11: Contour Plot of ED vs a_p vs f

Table 6: ANOVA and percentage contributions for ED

Source	DF	Adj SS	Adj MS	F	P	% Cont.
a_p	2	0.087	0.043	1.37	0.42	21.7
f	2	0.119	0.059	1.87	0.34	29.7
v_c	2	0.131	0.065	2.07	0.32	32.8
Error	2	0.063	0.031			15.85
Total	8	0.401				100

relationship between feed rate (f) and depth of cut (ap) in relation to the ED.

Table 6 shows that cutting speed (v_c) contributed the largest proportion to the response variance at 32.8%; however, this contribution is not statistically significant, as indicated by a P-value of 0.326. Additionally, the error variance accounts for 15.8%, indicating other sources of variance that are not captured by the model.

3.3. Multi-Response Optimization

Multi-response optimization combines the 2 responses, SR and ED, into a single response called the Multi-Response Performance Index (MRPI)[37]. The weight values (W) are determined using the smaller-is-better approach, as defined in Eq.(4) and Eq.(5). The MRPI is then calculated according to Eq.(3). Table 7 presents the weight values for SR and ED (W_{SR} and W_{ED}) along with the resulting MRPI values.

The Taguchi main effect analysis using MRPI values with the larger-is-better approach is shown in Figure 12. The contour plot shown in Figure13 demonstrates the relationship between f and ap in relation to MRPI. The most dominant factor affecting is the feed rate (f) and error contribution is significant =14.4% as shown in Table 8. The predicted optimal factor levels are ap = 0.8, f = 0.075, and vc = 200, with an S/N ratio of -4.325 and a mean value of 401.58 as shown in Table 9. The parameter level selection based on MRPI aligns consistently with the results in Figure 7 and Figure 9.

Table 9 presents the comparison between the predicted and experimental results for SR, ED, and MRPI, based on the selected criteria.

The predicted SR value was +2.84, while the experimental value was +3.05, resulting in a small error of +0.21 µm.

Table 7: The Multi Response Performance Index (MRPI)

Exp. No	SR	W_{SR}	ED	W_{ED}	MRPI
1	3.050	0.046	0.72	0.023	0.157
2	4.093	0.025	0.03	10.969	0.465
3	4.270	0.023	0.26	0.170	0.146
4	3.173	0.042	0.22	0.237	0.188
5	4.107	0.025	0.27	0.166	0.149
6	3.527	0.034	0.52	0.043	0.145
7	4.073	0.025	0.21	0.276	0.163
8	4.540	0.020	0.04	8.778	0.417
9	4.757	0.019	0.15	0.549	0.171

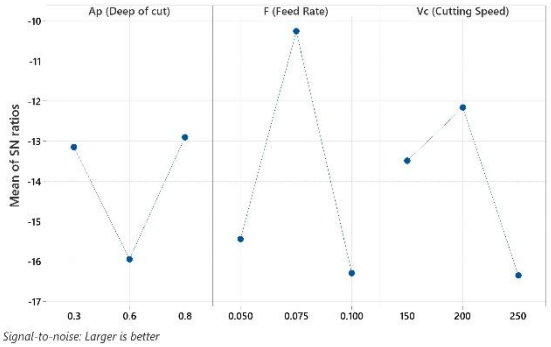

Fig. 12: Main Effect Plot for S/N ratios with MRPI

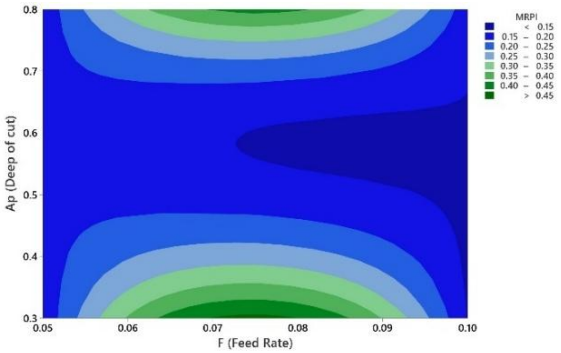

Fig. 13: Contour Plot of MRPI vs a_p vs f

Table 8: ANOVA and percentage contributions for MRPI

Source	DF	Adj SS	Adj MS	F	P	% Cont.
a_p	2	0.017	0.008	0.95	0.51	13.6
f	2	0.066	0.033	3.70	0.21	52.8
v_c	2	0.023	0.011	1.32	0.43	18.4
Error	2	0.018	0.009			14.4
Total	8	0.125				100

Table 9: Prediction S/N Ratios and Mean

a_p	f	v_c	S/N Ratio	Means
0.8	0.075	200	-4,325	401,58

This slight difference indicates that the model prediction closely aligns with the experimental results, especially for Exp.01 condition.

Table 10: Comparison Predicted vs Experimental Value

Criteria	SR Smaller-the-better	ED Smaller-the-better	MRPI Larger-the-better
a_p, f, v_c	0.6,0.05,150	0.8,0.075,200	0.8,0.075,200
Predict	+2.84	-0.16	NA
Exp.	+3.05	+0.09	SR = +4.722 ED= + 0.09
Error	+0.21	-0.07	---

The predicted ED value is -0.16 µm, while the experimental value is +0.09 µm, leading to an error of -0.07 µm. The discrepancy here indicates the occurrence of overcutting during the machining process, causing a slight increase in ED from the predicted value.

The MRPI value is presented in the experimental results as SR = +4.722 and ED = +0.09. However, the performance of MRPI may be subject to error due to the significant impact of ED, as MRPI is a composite of both SR and ED values. Additionally, the consistency of the results across trials remains difficult to establish.

3.4. Minimum Quantity Lubrication

Figure 14 illustrates the validation results comparing the machining processes conducted with and without the application of MQL. The MQL implementation significantly improved the SR compared to dry machining conditions. Specifically, the maximum SR achieved under MQL was 4.36 µm, representing a notable reduction compared to the 6.10 µm observed under dry conditions.

In the insert shown in Figure 11, it can be seen through the microscopy camera that the groove pattern with MQL usage is more regular marks and does not leave sticking.

In Figure 15 presents an SEM-based visual comparison between finished products with and without MQL-VCO at 2000× magnification. The surface produced without MQL exhibits a rough and irregular topography characterized by deep grooves, microcracks, and smeared layers of the plastically deformed material. These features indicate severe frictional interaction between the tool and the workpiece during machining, which likely generated excessive heat due to the absence of sufficient lubrication and cooling. The elevated temperature promotes local adhesion and plastic flow of the work material, resulting in built-up edges (BUE) and surface tearing. Consequently, the integrity of the surface layer deteriorates, and the SR increases significantly.

Fig. 14: Comparison of product finishing with MQL

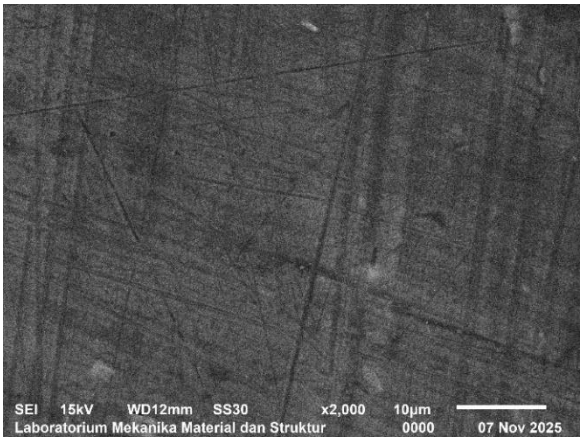

(a) Results on the surface with MQL

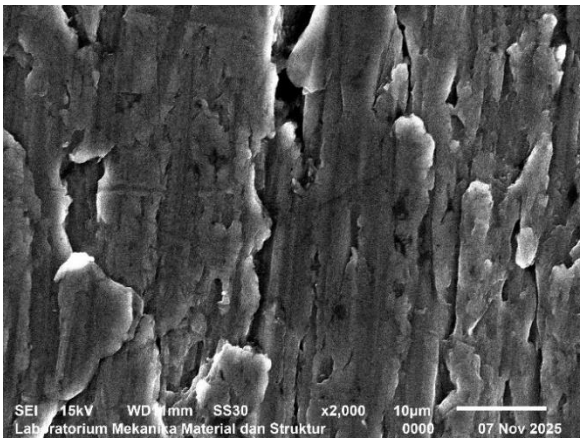

(b) Results on the surface without MQL

Fig. 15: Comparison of product finishing with SEM

3.5. Vibration

As shown in Figure 16 (a), the vibration amplitude gradually decreases as the cutting tool advances axially into the workpiece. This behavior indicates that the reduction in vibration is primarily caused by the increased structural stiffness of the workpiece as the effective overhang length decreases. The FFT spectrum obtained from the Experimental Modal Analysis (EMA), presented in Figure 16 (b), identifies the natural frequency of the workpiece at approximately 2230 Hz. Furthermore, as illustrated in Figure 16 (c), the short-time Fourier transform (STFT) analysis confirms the absence of significant frequency peaks near 2230 Hz throughout the machining process. These results indicate that the system maintained dynamic stability and that the cutting operation proceeded under chatter-free conditions.

4. Discussion

An analysis from a TRIZ-based perspective indicates that a higher feed rate (f) can improve the SR; however, it also

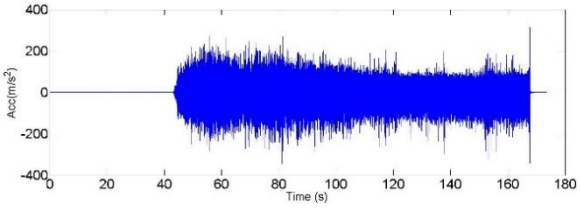

(a) Vibration during internal turning

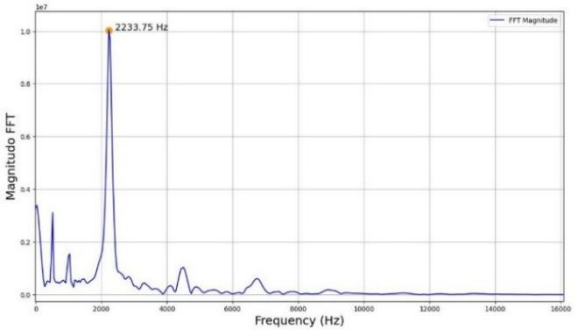

(b) FFT spectrum of the workpiece

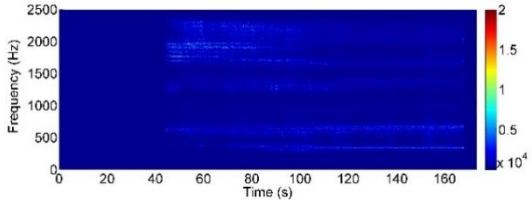

(c) Time-Frequency domain (STFT)

Fig. 16: Vibration Process

increases the cutting force (Fc), which may cause deflection of the boring bar and consequently lead to greater ED. Repeated deflection during machining can trigger chatter, a form of self-excited vibration resulting from the interaction between the cutting forces and the oscillating workpiece surface. This condition may lead to resonance when the vibration frequency approaches the natural frequency of the system.

To resolve this contradiction, in addition to selecting appropriate machining parameters, the application of lubrication can reduce F_c, thereby helping to achieve more optimal SR and ED. In the context of the Ideal Final Result (IFR), the application of the MRPI method for selecting cutting parameters can optimize SR and ED while minimizing chatter vibrations, without the need to increase the structural stiffness or modify the existing machine conditions.

MRPI is ineffective due to its high error contribution as shown in Table 8, with the feed rate (f), depth of cut (a_p), and cutting speed (v_c) being the key influencing parameters. The comparison results in Table 10 show that feed rate (f) has the most significant effect on SR, followed by depth of cut (a_p) and cutting speed (v_c), but these findings are consistent with experimental results that indicate the ineffectiveness of MRPI.

MQL with vegetable-based cutting oil improved SR, ED, and reduced chatter. The preliminary trial showed that the condition with MQL differed significantly, making it irrelevant to be used as a response for deep analysis. Virgin coconut oil prevents the cutter tip from sticking to the aluminum and reduces the cutting force (F_c). Under MQL with VCO, all processes operated with minimal chatter, as observed from the regularity of the results in the STFT plot. The effect of vibration has not yet caused chatter due to the reduction in the cutting force (F_c).

In Table 11 the comparison results of several references related to the main effect S/N ratio for the SR response are presented. It can be seen that the factor feed rate (f) has a dominant influence, followed by depth of cut (a_p) and the cutting speed (v_c). These results are in similarity with the experimental study that has been conducted Comparison results in Table 11 show feed rate (f) (a_p) (v).

Table 12, it can be seen that no studies have been found concerning the main effect S/N ratio for machining process factors with the ED response in the turning process. Some studies used cylindricity and roundness as responses. Only one study in the drilling process used the ED response, which cannot be compared. This indicates that

Table 11: Main effect of cutting parameters on SR

Reference	Process Machining	Workpiece	Main effect		
			a_p	f	v_c
Alaba at al. 2023 [48]	Wet external-turning using kernel oil	AISI 1039	2	1	3
Mastan (2023) [34]	Dry external-turning	Inconel 718	3	1	2
Maneesh (2023) [49]	Dry external-turning	Al-bronze	2	1	3
Sobh (2023) [50]	Dry external-turning	Ti-alloy TC21	1	2	3
Ramana (2023) [51]	Dry external-turning	Nickel A286	2	1	3
Dutta (2021) [52]	Dry external-turning	Additive Alloy	2	1	3
Kittali (2022) [53]	Wet external-turning	Alloy Steel EN1	2	1	3

Table 12: Main effect of cutting parameters on error geometric

Reference	Process Machining	Geometric Error	Main effect		
			a_p	f	v_c
Kurt (2009) [54]	Dry drilling on AA-2024	Error Diameter	3	1	2
Lin (2024) [55]	Dry internal-turning on S45C	Cylindricity	---	1	2
Kalyanakumar (2020) [42]	Wet and dry internal-turning on EN24	Roundness	3	2	1
Tiwari (2023) [56]	Dry vertical boring on Mild Steel	Roundness	2	1	3

the selection of the response for the ED needs to be further considered. VCO demonstrates thermal stability up to approximately 200 °C, making it suitable for light machining operations such as those involving aluminum alloys. Its chemical composition, which is rich in lauric and myristic acids, provides superior boundary lubrication characteristics that effectively reduce friction at the tool–workpiece interface[16,57]. This behavior contrasts with conventional flood cooling, which primarily serves to dissipate heat rather than enhance lubrication performance. Compared to mineral oils, VCO exhibits a relatively similar viscosity. Viscosity is an essential property of cutting fluids that significantly affects machining productivity. However, the rate of viscosity reduction in VCO with increasing temperature is slower than that of the mineral oils. Consequently, as the temperature decreases, VCO remains more fluid, preventing sticky residues on the workpiece and machine surfaces, and facilitating easier chip removal and cleaning.

In addition, VCO possesses a higher flash point than mineral oils, which helps minimize smoke formation under elevated temperature conditions[57]. This property not only reduces the risk of operator inhalation exposure but, owing to its biodegradable nature, also ensures better biocompatibility and environmental safety.

From an economic standpoint, the cost per liter of VCO is approximately one-fifth that of the mineral oil. When applied under MQL, the low fluid consumption results in a significant reduction in hourly operational costs. Meanwhile, due to its lower viscosity, mineral oil performs slightly better under lower air pressure requirements to achieve the same flow rate.

The application of MQL-VCO is highly suitable for industries using lightweight materials such as aluminum. In addition to the relatively low frictional heat generated between the tool and the workpiece, the spray pressure from the MQL-VCO system effectively prevents the formation of a build-up edge (BUE) on the cutting tool. This technology demonstrates strong potential for large-scale implementation, particularly in the automotive, electronics, and aerospace industries, and can be seamlessly integrated into existing CNC systems to promote sustainable manufacturing practices.

5. Conclusions

This study investigated the effects of machining parameters on the surface roughness (SR) and diameter error (ED) during the machining of thin-walled aluminum alloy 6063 under minimum quantity lubrication. The conclusion of this study is as follows:

SR and ED in thin-walled AA 6063 machining under MQL are strongly affected by machining parameters, with ED showing additional variability beyond the model's capture. Consequently, MRPI becomes less effective for multi-objective optimization due to the ED contribution

The ED is highly sensitive to setup accuracy, mainly due to reliance on nominal diameters from external measurement systems during initialization. Contributing factors include oval or tapered geometry, tool contact inaccuracies, misalignment, run-out, and deformation from tool pressure. Future studies are advised to use a 4-jaw chuck for better centering and to develop custom soft jaws to improve tool–workpiece contact and minimize setup-related errors.

Adjustments in the process parameters significantly affect machining dynamics, as indicated by the reduction in vibration amplitude and dominant frequency, reflecting changes in dynamic stiffness along the feed direction. The application of MQL-VCO reduces cutting force (F_c), enabling the use of higher process parameters, resulting in faster, more stable machining with no chatter and improved surface roughness (SR) quality.

The proposed MQL–VCO system demonstrates a high potential for scalability, indicating that it can be easily integrated into existing industrial machining lines without requiring major modifications. The implementation only requires the addition of an MQL nozzle and the use of standard compressed air pressure. Compared to conventional flood cooling systems that rely on pumps and coolant storage tanks, the MQL–VCO approach significantly reduces operational costs[58].

Acknowledgements

This research was funded by the in-house program "Teknologi Manufaktur Industri Berbasis Sumber Daya Lokal" at the Research Organization for Energy and Manufacture, National Research and Innovation Agency (BRIN) in 2025, under Decree No. B-1432/III.3.3/KU.01.02/3/2025. It was also supported by the LPDP–RIIM Grant of the National Research and Innovation Agency (BRIN), under Decree Nos. B802/II.7.5/FR/6/2022 and B9106/III.3/KS.0.0/9/2022, as well as through the Degree by Research Program under Decree No. 27/II/HK/2024, for which the authors express their sincere appreciation and gratitude.

Nomenclature

AA-6063	aluminum alloy 6063
Acc	vibration from the accelerometer (m/s^2)
ANOVA	analysis of variance
a_p	depth of cut (mm)
Box	box-behnken design
CCD	central composite design
Ce	circularity error
CMM	coordinate measuring machine
Dd	desire internal diameter (mm)
DEAR	deviation-based evaluation of the alternating responses
DF	degree of freedom

Di	inner diameter (mm)
Do	outer diameter (mm)
DOE	desain of experiment
ED	diameter error (mm)
EMA	experiment modal analysis
Exp.No	experiment number (-)
Ext	external
f	nominal feed rate (mm/rev)
F_c	cutting force (N)
Fz	force axial
FFT	fast fourier transform
fr	feed (mm/min)
GA	genetic algorithm
GRA	grey relation analysis
IFR	ideal final result
L_9	taguchi 9 ortogonal array (-)
LCA	Life Cycle Assessment
L/D	long/ diameter ratio (-)
MOGWO	multi-objective grey wolf optimizer.
MOORA	multi-objective optimization by ratio analysis
MOPSO	multi-objective particle swarm optimization
MRPI	multi response performance index (-)
MRR	material removal rate (mm^3/min)
MS	mean square
MQCL	minimum quantity cooling lubricant
MQL	minimum quantity lubrication
NSGA-II	non-dominated sorting genetic algorithm II
Pc	power consumption
RSM	response surface methodology
S/N ratio	signal/ noise ratio (-)
SCE	specific cutting energy (J/mm^2)
SR	surface roughness - Ra (µm)
SS	sum of square
STFT	short time fourier transform
tf	thinkness finishing (mm)
T-GRA	taguchi-grey relational analysis
to	thickness start (mm)
TOPSIS	technique for order preference by similarity to ideal solution
TRIZ	theory of inventive problem solving
T_w	tool wear (V_b)
T_{wr}	tool wear rate
VCO	virgin coconut oil
v_c	cutting speed (m/min)
V_{ib}	vibration
WCS	workpiece coordinate system
W_{ED}	weight diameter error (-)
W_{SR}	weight surface roughness (-)
Y_{ED}	diameter error responds (mm)
Y_{SR}	surface roughness responds (µm)

References

1) I. Asiltürk, and H. Akkuş, "Determining the effect of cutting parameters on surface roughness in hard turning using the taguchi method," Measurement (Lond), 44 (9) 1697–1704 (2011). doi: 10.1016/j.measurement.2011.07.003.
2) J. Eapen, S. Murugappan, and S. Arul, "A Study on Chip Morphology of Aluminum Alloy 6063 during Turning under Pre Cooled Cryogenic and Dry Environments-review under responsibility ofthe Committee Members of International Conference on Advancements in Aeromechanical Materials for Manufacturing (ICAAMM-2016)," 2017. www.sciencedirect.comwww.materialstoday.com/proceedings.
3) J. Du, K. Liu, Z. Feng, C. Xu, and P. Hao, "Investigation on crashworthiness of lightweight thin-walled protective structure of mav inspired by beetle exoskeleton," Mechanics of Advanced Materials and Structures, 31 (26) 8169–8179 (2024). doi:10.1080/15376494.2023.2255171.
4) F.A.R. Rozhbiany, and S.R. Jalal, "Reinforcement and processing on the machinability and mechanical properties of aluminum matrix composites," Journal of Materials Research and Technology, 8 (5) 4766–4777 (2019). doi: 10.1016/j.jmrt.2019.08.023.
5) A. Krisbudiman, K. Rezqi, R.L. Gumilang, M. Dahsyat, H. Zenal, A.M. Kadir, and E. Yulianto, "Structural design analysis torque links of nose landing gear on light aircraft," International Journal on Advanced Science, Engineering and Information Technology, Vol. 14, No. 2, Apr. 2024, 14 (2) (2024). doi:10.18517/ijaseit.14.2.19317.
6) H. Manikandan, and T. Chandra Bera, "Modelling of dimensional and geometric error prediction in turning of thin-walled components," Precis Eng, 72 382–396 (2021). doi: 10.1016/j.precisioneng.2021.05.013.
7) Y. Altintas, D. Lappin, D. van Zyl, and D. Östling, "Automatically tuned boring bar system," CIRP Annals, 70 (1) 313–316 (2021). doi: 10.1016/j.cirp.2021.04.058.
8) A. Susanto, M. Azka, K. Yamada, K. Sekiya, P. Novia, R. Tanaka, and M.D. Prasetio, "Analysis of Transient Signal using Hilbert-Huang Transform for Chatter Monitoring in Turning Process," 2019.
9) D. van Zyl, Y. Altintas, and D. Ostling, "Parametric design of boring bars with adaptive tuned mass dampers," CIRP J Manuf Sci Technol, 38 491–499 (2022). doi: 10.1016/j.cirpj.2022.06.003.
10) G. Quintana, and J. Ciurana, "Chatter in machining processes: a review," Int J Mach Tools Manuf, 51 (5) 363–376 (2011). doi: 10.1016/j.ijmachtools.2011.01.001.
11) M. Eynian, and Y. Altintas, "Chatter stability of general turning operations with process damping," J Manuf Sci Eng, 131 (4) 0410051–04100510 (2009). doi:10.1115/1.3159047.
12) M.N. Derani, & Mani, and M. Ratnam, "The use of tool flank wear and average roughness in assessing effectiveness of vegetable oils as cutting fluids during turning-a critical review," The International Journal of Advanced Manufacturing Technology,

112 1841–1871 (2022). doi:10.1007/s00170-020-06490-5/Published.

13) J. Haider, and M.S.J. Hashmi, "Health and Environmental Impacts in Metal Machining Processes," in: Comprehensive Materials Processing: Thirteen Volume Set, Elsevier, 2014: pp. V8-7-V8-33. doi:10.1016/B978-0-08-096532-1.00804-9.
14) S. Akhai, "Navigating the potential applications and challenges of intelligent and sustainable manufacturing for a greener future," Evergreen, 10 (4) 2237–2243 (2023). doi:10.5109/7160899.
15) S. Ravi, P. Gurusamy, and V. Mohanavel, "A review and assessment of effect of cutting fluids," in: Mater Today Proc, Elsevier Ltd, 2020: pp. 220–222. doi: 10.1016/j.matpr.2020.05.054.
16) B.S. Ajay Vardhaman, M. Amarnath, D. Jhodkar, J. Ramkumar, H. Chelladurai, and M.K. Roy, "Influence of coconut oil on tribological behavior of carbide cutting tool insert during turning operation," Journal of the Brazilian Society of Mechanical Sciences and Engineering, 40 (9) (2018). doi:10.1007/s40430-018-1379-y.
17) A. Wahjudi, A.R. Yusoff, S. Sabil, B.O. P Soepangkat, S. Suhardjono, and P. Al-Sultan Abdullah, "A study of end milling process parameter's effect on thin wall aluminum-7075 surface roughness under minimum quantity lubrication," 2024.
18) X. Luo, S. Wu, D. Wang, Y. Yun, Q. An, and C. Li, "Sustainable development of cutting fluids: the comprehensive review of vegetable oil," J Clean Prod, 473 143544 (2024). doi: 10.1016/J.JCLEPRO.2024.143544.
19) A. Sharma, and R. Kumar, "Potential use of minimum quantity lubrication (MQL) in machining of biocompatible materials using environment friendly cutting fluids: An overview," in: Mater Today Proc, Elsevier Ltd, 2021: pp. 5315–5319. doi: 10.1016/j.matpr.2021.01.904.
20) C.L. He, W.J. Zong, and J.J. Zhang, "Influencing factors and theoretical modeling methods of surface roughness in turning process: state-of-the-art," Int J Mach Tools Manuf, 129 15–26 (2018). doi: 10.1016/j.ijmachtools.2018.02.001.
21) D. Chen, B. Lin, Z. Han, and Y. Zhang, "Study on the optimization of cutting parameters in turning thin-walled circular cylindrical shell based upon cutting stability," International Journal of Advanced Manufacturing Technology, 69 (1–4) 891–899 (2013). doi:10.1007/s00170-013-5073-z.
22) Z. Li, Z. Zeng, Y. Yang, Z. Ouyang, P. Ding, J. Sun, and S. Zhu, "Research progress in machining technology of aerospace thin-walled components," J Manuf Process, 119 463–482 (2024). doi: 10.1016/j.jmapro.2024.03.111.
23) A. Gerasimenko, M. Guskov, A. Gouskov, P. Lorong, and A. Shokhin, "Analytical modeling of a thin-walled cylindrical workpiece during the turning process. stability analysis of a cutting process," Journal of Vibroengineering, 19 (8) 5825–5841 (2017). doi:10.21595/jve.2017.18061.
24) B. Toubhans, P. Lorong, F. Viprey, G. Fromentin, and H. Karaouni, "A versatile approach, considering tool wear, to simulate undercut error when turning thin-walled workpieces," (n.d.). doi:10.1007/s00170-021-07243-8/Published.
25) M. Wan, H.N. Wang, and Y. Yang, "Dynamics of the truncated conical thin-wall turning process," J Manuf Process, 94 49–62 (2023). doi: 10.1016/j.jmapro.2023.03.059.
26) T. Aijun, and L. Zhanqiang, "Deformations of thin-walled plate due to static end milling force," J Mater Process Technol, 206 (1–3) 345–351 (2008). doi: 10.1016/j.jmatprotec.2007.12.089.
27) J. Falta, M. Sulitka, M. Janota, and V. Frkal, "Model of force interaction for stability prediction in turning of thin-walled cylindrical workpiece," International Journal of Advanced Manufacturing Technology, 125 (1–2) 195–212 (2023). doi:10.1007/s00170-022-10343-8.
28) P. Jayaraman, and L. Mahesh kumar, "Multi-response optimization of machining parameters of turning AA6063 T6 aluminium alloy using grey relational analysis in Taguchi method," in: Procedia Eng, Elsevier Ltd, 2014: pp. 197–204. doi: 10.1016/j.proeng.2014.12.242.
29) G. Singh, A. Kumar, V. Aggarwal, and S. Singh, "Experimental investigations and optimization of machining performance during turning of EN-31 steel using TOPSIS approach," in: Mater Today Proc, Elsevier Ltd, 2021: pp. 1089–1094. doi: 10.1016/j.matpr.2021.07.381.
30) F. Ziyad, H. Alemayehu, D. Wogaso, F. Dadi, and M. Badri, "Multi-objective optimization of machining parameters of mild steel aisi 1018 under compressed air-assisted cooling by using genetic algorithm," International Journal on Interactive Design and Manufacturing, 19 (7) 5291–5311 (2025). doi:10.1007/s12008-024-02134-0.
31) B. Sen, A. Bhowmik, N. Rachchh, N. Patil, A. Khatibi, and R. Kumar, "Exploring cryo-mql medium for hard machining of hastelloy c276: a multi-objective optimization approach," International Journal on Interactive Design and Manufacturing, (2024). doi:10.1007/s12008-024-02069-6.
32) M. Imran, S. Shuangfu, B. Yuzhu, W. Yuming, and N. Raheel, "Optimising subsurface integrity and surface quality in mild steel turning: a multi-

objective approach to tool wear and machining parameters," Journal of Materials Research and Technology, 35 3440–3462 (2025). doi: 10.1016/j.jmrt.2025.01.246.

33) T. Gopi, P.S. Goud, K. Abhishek, N. Sateesh, R. Karthikeyan, A. Kumar, and B.C.H. Nookaraju, "A hybrid multi-optimization of cutting rate and surface roughness using pca-based improved-gwo in precise cnc turning of aa2014," International Journal on Interactive Design and Manufacturing, 19 (6) 4113–4121 (2025). doi:10.1007/s12008-024-02031-6.
34) P. Mastan Rao, C. Deva Raj, S.H. Dhoria, M. Vijaya, and J.R.R. Chowdary, "Multi-objective optimization of turning for nickel-based alloys using taguchi-gra and topsis approaches," Journal of The Institution of Engineers (India): Series D, (2023). doi:10.1007/s40033-023-00554-y.
35) J.T. Vieira, R.B.D. Pereira, C.H. Lauro, L.C. Brandão, and J.R. Ferreira, "Multi-objective evolutionary optimization of extreme gradient boosting regression models of the internal turning of peek tubes," Expert Syst Appl, 238 (2024). doi: 10.1016/j.eswa.2023.122372.
36) M. Fan, G. Sun, J. Ding, and J. Song, "Investigation on multi-objective optimization for in-situ laser-assisted machining of glass-ceramic," Appl Phys A Mater Sci Process, 130 (10) (2024). doi:10.1007/s00339-024-07911-y.
37) Y. Şahin, and D. Akbar, "Multi-response optimization in cutting mild steels," Applied Chemical Engineering, 7 (1) (2023). doi:10.24294/ace.v7i1.2599.
38) A.D. Tura, E.O. Isaya, U.L. Adizue, B.Z. Farkas, and M. Takács, "Optimization of ultra-precision cbn turning of aisi d2 using hybrid ga-rsm and taguchi-gra statistic tools," Heliyon, 10 (11) e31849 (2024). doi: 10.1016/J.HELIYON. 2024.E31849.
39) Janet. Evanovich, and Lorelei. King, "Optimization of surface roughness, tool wear and material removal rate in turning of inconel 718 with ceramic composite tools using mcdm methods based on taguchi methodology," Sadhana - Academy Proceedings in Engineering Sciences, 48 (2022).
40) K. Safi, M.A. Yallese, S. Belhadi, T. Mabrouki, and A. laouissi, "Tool wear, 3d surface topography, and comparative analysis of gra, moora, dear, and waspas optimization techniques in turning of cold work tool steel," International Journal of Advanced Manufacturing Technology, 121 (1–2) 701–721 (2022). doi:10.1007/s00170-022-09326-6.
41) G.R. Chate, M.P. Manjunath, H. H.m., S.U. Urankar, S.A. Sanadi, A.P. Jadhav, S. Hiremath, and A.S. Deshpande, "Sustainable machining: Modelling and optimization using Taguchi, MOORA and DEAR methods," in: Mater Today Proc, Elsevier Ltd, 2021: pp. 8941–8947. doi: 10.1016/j.matpr.2021.05.365.
42) S. Kalyanakumar, S.T. Chandy, K.T. Adil Muhammed, and P.S. Rohith, "Multi-response optimization of machining parameters of turning operation with green environment in EN24T using grey relational analysis in Taguchi method," in: Mater Today Proc, Elsevier Ltd, 2020: pp. 6193–6197. doi:10.1016/j.matpr.2020.10.508.
43) D. Sarma, J. Borah, and M. Chandrasekaran, "Multi optimization of nano fluid based machining of titanium alloy: A green manufacturing approach," in: Mater Today Proc, Elsevier Ltd, 2021: pp. 8921–8926. doi: 10.1016/j.matpr.2021.05.362.
44) C. Moganapriya, & R. Rajasekar, & T. Mohanraj, V.K. Gobinath, & P. Sathish Kumar, and C. Poongodi, "Dry machining performance studies on tialsin coated inserts in turning of aisi 420 martensitic stainless steel and multi-criteria decision making using taguchi - dear approach," Silicon, 14 (2021). doi:10.1007/s12633-021-01202-4/Published.
45) V.V.K. Lakshmi, K.V. Subbaiah, A.V. Kothapalli, and K. Suresh, "Parametric optimization while turning ti-6al-4v alloy in mist-mqcl (green environment) using the dear method," Manuf Rev (Les Ulis), 7 (2020). doi:10.1051/mfreview/2020034.
46) A.S. Wadhwa, M. Abbass, S. Akhai, D. Kumar, and P. Kumar, "Integrating Taguchi optimization for multi-criteria decision making in engineering applications," in: Recent Theories and Applications for Multi-Criteria Decision-Making, IGI Global, 2024: pp. 125–150. doi:10.4018/979-8-3693-6502-1.ch005.
47) S.H. ALI, Y. YAO, B. WU, B. ZHAO, W. DING, M. JAMIL, A. KHAN, A. BAIG, Q. LIU, and D. XU, "Recent developments in mql machining of aeronautical materials: a comparative review," Chinese Journal of Aeronautics, 38 (1) (2025). doi: 10.1016/j.cja.2024.01.018.
48) E.S. Alaba, R.A. Kazeem, A.S. Adebayo, M.O. Petinrin, O.M. Ikumapayi, T.C. Jen, and E.T. Akinlabi, "Evaluation of palm kernel oil as cutting lubricant in turning aisi 1039 steel using taguchi-grey relational analysis optimization technique," Advances in Industrial and Manufacturing Engineering, 6 (2023). doi: 10.1016/j.aime.2023.100115.
49) K. Maneesh, M. Shan, S. Xavier, M.B. Vinayak, and M. Shafeek, "Quality characteristic optimization in CNC turning of aluminum bronze by using Taguchi's approach and ANOVA," in: Mater Today Proc, Elsevier Ltd, 2023: pp. 620–628. doi: 10.1016/j.matpr.2022.11.059.
50) A.S. Sobh, E.M. Sayed, A.F. Barakat, and R.N. Elshaerr, "Turning parameters optimization for tc21 ti-alloy using taguchi technique," Beni Suef Univ J

Basic Appl Sci, 12 (1) (2023). doi:10.1186/s43088-023-00356-x.

51) M.V. Ramana, G.K. Mohana Rao, B. Sagar, R.K. Panthangi, and B.V.R. Ravi Kumar, "Optimization of surface roughness and tool wear in sustainable dry turning of iron based nickel a286 alloy using taguchi's method," Clean Eng Technol, 2 (2021). doi: 10.1016/j.clet.2020.100034.
52) S. Dutta, and S. Kumar Reddy Narala, "Optimizing turning parameters in the machining of am alloy using taguchi methodology," Measurement (Lond), 169 (2021). doi: 10.1016/j.measurement.2020.108340.
53) P. Kittali, V. Kalwa, D. Athith, K.P. Prashanth, and B.K. Venkatesh, "Optimization of machining parameters in turning operation to minimize the surface roughness using taguchi technique for en1a alloy steel," Mater Today Proc, 54 463–467 (2022). doi: 10.1016/j.matpr.2021.10.323.
54) M. Kurt, E. Bagci, and Y. Kaynak, "Application of taguchi methods in the optimization of cutting parameters for surface finish and hole diameter accuracy in dry drilling processes," International Journal of Advanced Manufacturing Technology, 40 (5–6) 458–469 (2009). doi:10.1007/s00170-007-1368-2.
55) Y.F. Lin, P.Y. Lai, G.Y. Chen, and Z.P. Zhang, "Optimization of surface roughness and cylindricity using the taguchi method in boring of s45c steel with tungsten steel and phosphor bronze damping materials," International Journal of Advanced Manufacturing Technology, (2024). doi:10.1007/s00170-024-14796-x.
56) V. Tiwari, A. Bansal, A. Kaushik, and U. Punia, "Optimization of jig boring process parameter by taguchi approach," Mater Today Proc, (2023). doi: 10.1016/j.matpr.2023.02.051.
57) E. Kuram, B. Ozcelik, and E. Demirbas, "Environmentally Friendly Machining: Vegetable Based Cutting Fluids," in: 2013: pp. 23–47. doi:10.1007/978-3-642-33792-5_2.
58) N. Khanna, P. Shah, M. Sarikaya, and F. Pusavec, "Energy consumption and ecological analysis of sustainable and conventional cutting fluid strategies in machining 15–5 phss," Sustainable Materials and Technologies, 32 (2022). doi: 10.1016/j.susmat. 2022.e00416.